

min. Solutions (and the atmosphere above them) of NO were colorless in the three solvents used. After the introduction of NO, the platinum working electrode was inserted and the cell sealed. The gain on the potentiostat was set to that of the known concentration of  $\text{NO}^+\text{BF}_4^-$  in the particular solvent. At these settings, the concentration of NO was adjusted to give currents nearly the same as that obtained from a  $1 \times 10^{-2}$  M  $\text{NO}^+$  solution. Decreasing the concentration of NO was simply performed by allowing argon to flow through the CV cell for a short period of time. This process was repeated until the currents were roughly similar to those of the  $\text{NO}^+$  solutions in a given solvent and at the same scan rate. For the solvents  $\text{CH}_3\text{CN}$  and  $\text{NO}_2\text{Me}$ , the voltammograms showed clean diffusive behavior (see Table II). However, in the cyclic voltammogram of NO in dichloromethane, adsorption at the platinum working electrode was apparent for both the oxidation of NO and the return  $\text{NO}^+$  reduction waves at concentrations greater than  $\sim 5 \times 10^{-3}$  M. Even at concentrations of  $< 5 \times 10^{-3}$  M, slight adsorption effects were indicated by the nonconstant  $i_p/\sqrt{v}$  values shown in Table II. The adsorption was only minor, since the CV waves continued to be rather diffusive in character, as shown in Figure 2C. The adsorption effects were not taken into account in the calculation of the heterogeneous charge-transfer rate,  $k_s$ . Thus, these values in Table III must be accepted with some caution.

**Activation Barriers for Electron Transfer.** The heterogeneous rate constants  $k_s$  in Table III were related to the activation free energy<sup>52</sup> as  $k_s = \kappa A \exp(-\Delta G_{el}^\ddagger/kT)$ , where  $\kappa$  for the transmission coefficient is taken

as unity, and the preexponential factor  $A = (\delta r_e) \Gamma_n \nu_n$  was evaluated as  $3 \times 10^5 \text{ cm s}^{-1}$  for  $\Gamma_n = 1$ ,  $\delta r_e = 1 \times 10^{-8} \text{ cm}$ , and  $\nu_n = 3 \times 10^{13} \text{ s}^{-1}$ .<sup>70</sup> The correction for the charging of the double layer<sup>71</sup> was neglected by assuming that the electrode potential was close to the bulk potential,<sup>46,54</sup> the difference being approximated as no more than 15%.<sup>58,72</sup> The inner-sphere reorganization energy was approximated by the Marcus relationship<sup>73,74</sup>  $\lambda_i = [\sum f_j^O f_j^R / (f_j^O + f_j^R)] (\Delta r)^2$ , where  $f_j^O$  and  $f_j^R$  are the force constants of the oxidized  $\text{NO}^+$  ( $\text{O}_2$ ) and the reduced NO ( $\text{O}_2^-$ ) respectively.

**Acknowledgment.** We thank Professors D. K. Gosser and P. H. Rieger for kindly providing the computer program<sup>26</sup> for CV simulation, C. Amatore for helpful discussion, and the National Science Foundation, Texas Advanced Research Program, and Robert A. Welch Foundation for financial support.

- (70) See: Hupp, J. T.; Weaver, M. J. *J. Electroanal. Chem. Interfacial Electrochem.* **1983**, *152*, 1.  
 (71) Frumkin, A. N. *Z. Phys. Chem., Abt. A* **1933**, 121.  
 (72) (a) Gennet, T.; Milner, D. F.; Weaver, M. J. *J. Phys. Chem.* **1985**, *89*, 2787. (b) Gennet, T.; Weaver, M. J. *J. Electroanal. Chem. Interfacial Electrochem.* **1985**, *186*, 179.  
 (73) The outer-sphere reorganization energies of  $\text{NO}^+/\text{NO}$  and  $\text{O}_2/\text{O}_2^-$  (of similar sizes and charge) are likely to be similar.  
 (74) Marcus, R. A. *J. Phys. Chem.* **1963**, *67*, 853.

Contribution from the Institute of Physical and Chemical Research, Wako-shi, Saitama 351-01, Japan

## Reaction of (Dioxygen)(dithiocarbamato)rhodium Complexes with Carbon Dioxide. Formation and Chemical Cleavage of Rhodium Peroxycarbonato and Carbonato Rings

Yasuo Wakatsuki,\* Masahiro Maniwa,<sup>†</sup> and Hiroshi Yamazaki

Received February 27, 1990

Dioxygen complexes of bis(triphenylphosphine)(dithiocarbamato)rhodium and its analogue have been prepared. The structure determined by NMR spectroscopy was interpreted by the strong electron-accepting nature of the dioxygen ligand. The complex reacts with carbon dioxide at room temperature to give the peroxycarbonato complex  $\text{Rh}(\text{S}_2\text{CNMe}_2)(\text{CO}_4)(\text{PPh}_3)_2$ . The structure of this complex, in which the oxygen atom originating from carbon dioxide occupies the position trans to one of the S atoms of the chelating  $\text{S}_2\text{CNMe}_2$  while the oxygen originating from the dioxygen is trans to one of the  $\text{PPh}_3$  ligands, is proposed on the basis of its successive reactions. In the presence of excess triphenylphosphine, the peroxycarbonato was deoxygenated to give a yellow carbonato complex,  $\text{Rh}(\text{S}_2\text{CNMe}_2)(\text{CO}_3)(\text{PPh}_3)_2$ , which has two trans(S,O) pairs and trans triphenylphosphines, as characterized by crystallographic analysis. The complex crystallizes in the triclinic system, space group  $P\bar{1}$ , with  $a = 12.634$  (5) Å,  $b = 17.681$  (4) Å,  $c = 10.449$  (4) Å,  $\alpha = 98.97$  (3)°,  $\beta = 109.27$  (4)°,  $\gamma = 99.27$  (2)°, and  $Z = 2$ . When heated to 70 °C, this complex isomerizes to the thermodynamically stable form with an orange-red color. After being heated for a prolonged time in the presence of triphenylphosphine, the carbonato complex was further deoxygenated to give the carbon dioxide adduct of  $\text{Ru}(\text{S}_2\text{CNMe}_2)(\text{PPh}_3)_2$ , which was not isolated but characterized by NMR spectroscopy.

### Introduction

Although a variety of group VIII metal peroxy complexes have been prepared from dioxygen, they are in general reluctant to react with simple olefins by nonradical pathways. A notable exception is the case of rhodium:  $[\text{Rh}(\text{O}_2)(\text{AsPh}_3)_4]^+$  can transfer its oxygen ligand to terminal olefins, producing ketones.<sup>1</sup> The combination of rhodium chloride and cupric perchlorate in alcohol catalyzes oxidation of terminal olefins by  $\text{O}_2$  at room temperature.<sup>2</sup> It appears, therefore, important to understand the reactivity of the dioxygen molecule coordinated to rhodium. To our knowledge, only two mononuclear rhodium-dioxygen complexes,  $[\text{Rh}(\text{O}_2)(\text{AsMe}_2\text{Ph})_4]\text{ClO}_4$ <sup>1</sup> and  $\text{RhCl}(\text{O}_2)(^t\text{BuNC})(\text{PPh}_3)_2$ ,<sup>3</sup> and two dinuclear complexes,  $[\text{RhCl}(\text{O}_2)(\text{PPh}_3)_2]_2$ <sup>4</sup> and  $[\text{Rh}(\text{cod})]_2(\text{O}_2)$ ,<sup>5</sup> have been known, but reactivity of the coordinating dioxygen has not been fully examined. In this report we describe the preparation of a mononuclear rhodium-dioxygen complex having dithiocarbamate and triphenylphosphine as ancillary ligands. Its reaction with carbon dioxide is fairly facile and provides information concerning reactivity and bonding of the oxygen atoms bound to

rhodium. The present work is also relevant to the recent literature that addition of carbon dioxide affects the product distribution in the Rh(I)-catalyzed oxidation of styrene by  $\text{O}_2$ .<sup>6</sup>

### Experimental Section

<sup>1</sup>H and <sup>31</sup>P NMR spectra were recorded on a JEOL JNM-GX-400 spectrometer in  $\text{CD}_2\text{Cl}_2$  using  $\text{SiMe}_4$  and  $\text{H}_3\text{PO}_4$  as internal and external standards, respectively. IR spectra were obtained on a Shimadzu IR-27G spectrometer using the KBr pellet method. For column chromatography, Sumitomo activated alumina KCG-30, deactivated beforehand by 10 wt % of water, or WAKOGEL C-200 was used.

**Preparation of  $\text{Rh}(\text{S}_2\text{CNMe}_2)(\text{O}_2)(\text{PPh}_3)_2$  (2a).** A mixture of  $\text{RhCl}(\text{PPh}_3)_3$  (1 g, 1.2 mmol), Na(dtc) (dtc = dimethyldithiocarbamate; 194 mg, 1.1 mmol), and triphenylphosphine (288 mg, 1.1 mmol) in THF

<sup>†</sup> Waseda University exchange fellow.

- (1) Igersheim, F.; Mimoun, H. *Nouv. J. Chim.* **1980**, *4*, 161.  
 (2) Mimoun, H.; Perez Hachirant, M. M.; Serec de Roch, I. *J. Am. Chem. Soc.* **1978**, *100*, 5437.  
 (3) Nakamura, A.; Tatsuno, Y.; Otsuka, S. *Inorg. Chem.* **1972**, *11*, 2058.  
 (4) Bennet, N.; Donaldson, R. *J. Am. Chem. Soc.* **1971**, *93*, 3307.  
 (5) Sakurai, F.; Suzuki, H.; Moro-oka, Y.; Ikawa, T. *J. Am. Chem. Soc.* **1980**, *102*, 1749.  
 (6) Aresta, A.; Quaranta, E.; Ciccarese, A. *J. Mol. Catal.* **1987**, *41*, 355.

Table I. Crystallographic Data for **5**

$C_{40}H_{36}NO_3P_2RhS_2 \cdot CH_2Cl_2$	$V = 2119 (1) \text{ \AA}^3$
$f_w = 807.7$	$Z = 2$
cryst class: triclinic	$T = 20 \text{ }^\circ\text{C}$
space group: $P\bar{1}$	$\lambda = 0.7107 \text{ \AA}$
$a = 12.634 (5) \text{ \AA}$	$\rho_c = 1.266 \text{ g}\cdot\text{cm}^{-3}$
$b = 17.681 (4) \text{ \AA}$	$\mu(\text{Mo K}\alpha) = 2.26 \text{ cm}^{-1}$
$c = 10.449 (4) \text{ \AA}$	cryst size: $0.31 \times 0.25 \times 0.20 \text{ mm}$
$\alpha = 98.97 (3)^\circ$	$R = 0.069$
$\beta = 109.27 (4)^\circ$	$R_w = 0.100$
$\gamma = 99.27 (2)^\circ$	

(40 mL) was stirred for 20 min. After evaporation of the solvent, the residue was chromatographed on alumina and a yellow-orange band of  $\text{Rh}(\text{S}_2\text{CNMe}_2)(\text{PPh}_3)_2$  (**1a**) was eluted with benzene. Triphenylphosphine (280 mg) was added to the eluate, and the mixture was slowly bubbled with dioxygen gas for 30 min. The reaction mixture was concentrated to ca. 10 mL, and hexane was added to give brown microcrystals of **2a** (87% yield). Mp: 248 °C dec. Anal. Calcd for  $\text{C}_{39}\text{H}_{36}\text{NO}_3\text{P}_2\text{RhS}_2 \cdot 0.5\text{C}_6\text{H}_6$ : C, 61.61; H, 4.80; N, 1.71. Found: C, 62.08; H, 4.89; N, 1.66.

**Preparation of  $\text{Rh}(\text{S}_2\text{CNMe}_2)(\text{O}_2)(\text{Ph}_4\text{P}_2\text{C}_2\text{H}_4)$  (**2b**).** A mixture of  $[\text{RhCl}(\text{dppe})_2]$  (dppe = 1,2-bis(diphenylphosphino)ethane; 50 mg, 0.047 mmol), Na(dtc) (17 mg, 0.094 mmol), and dppe (19 mg, 0.094 mmol) in THF (30 mL) was stirred for 1 h. The reaction mixture was worked up as in the case of **2a** above to give dark brown crystals of **2b** (31% yield). Mp: 248–250 °C dec. Recrystallization was unsuccessful. Anal. Calcd for  $\text{C}_{29}\text{H}_{30}\text{NO}_2\text{P}_2\text{RhS}_2 \cdot \text{C}_6\text{H}_6$ : C, 57.45; H, 4.96; N, 1.91. Found: C, 56.39; H, 4.87; N, 1.81.

**Preparation of  $\text{Rh}(\text{S}_2\text{CNMe}_2)(\text{CO}_4)(\text{PPh}_3)_2$  (**3a**) and  $\text{Rh}(\text{S}_2\text{CNMe}_2)(\text{CO}_4)(\text{dppe})$  (**3b**).** Through a solution of  $\text{Rh}(\text{S}_2\text{CNMe}_2)(\text{PPh}_3)_2$  (**1a**)<sup>7</sup> (70 mg, 0.094 mmol) and triphenylphosphine (25 mg, 0.094 mmol) in benzene (20 mL) were slowly bubbled carbon dioxide gas and dioxygen for 30 min. The yellow precipitate that formed was filtered out and washed with benzene. Recrystallization from  $\text{CH}_2\text{Cl}_2$ /hexane in the presence of  $\text{PPh}_3$  gave red crystals of **3a** (10% yield) and a small amount of yellow crystals of **5**, which were mechanically removed. Mp: 173–175 °C dec. Anal. Calcd for  $\text{C}_{40}\text{H}_{36}\text{NO}_4\text{P}_2\text{RhS}_2 \cdot 0.5\text{CH}_2\text{Cl}_2$ : C, 56.16; H, 4.31; N, 1.62. Found: C, 55.94; H, 4.37; N, 1.62. Complex **3b** was prepared by bubbling  $\text{CO}_2$  gas through a benzene solution containing **2b**. Mp: 263–265 °C dec. Anal. Calcd for  $\text{C}_{30}\text{H}_{30}\text{NO}_4\text{P}_2\text{RhS}_2 \cdot \text{CH}_2\text{Cl}_2$ : C, 47.58; H, 4.12; N, 1.79. Found: C, 47.31; H, 4.02; N, 1.76.

**Preparation of  $\text{Rh}(\text{S}_2\text{CNMe}_2)(\text{CO}_3)(\text{PPh}_3)_2$  (**5**).** A solution of **1a** (150 mg, 0.20 mmol) and  $\text{PPh}_3$  (78 mg, 0.30 mmol) in  $\text{CH}_2\text{Cl}_2$  (20 mL) was stirred under an atmosphere of dioxygen for 10 min and then was bubbled with a slow stream of carbon dioxide for several minutes. After 4 h, the solution was concentrated and hexane was added to give yellow crystals of **5** (88% yield), which were recrystallized from  $\text{CH}_2\text{Cl}_2$ /hexane. Mp: 167 °C dec. Anal. Calcd for  $\text{C}_{40}\text{H}_{36}\text{NO}_3\text{P}_2\text{RhS}_2 \cdot \text{CH}_2\text{Cl}_2$ : C, 55.17; H, 4.29; N, 1.57. Found: C, 54.66; H, 4.31; N, 1.49.

**Isomerization of **5** to **6**.** Complex **5** (70 mg, 0.087 mmol) and  $\text{PPh}_3$  (25 mg, 0.095 mmol) were dissolved in  $\text{CH}_2\text{Cl}_2$  (7 mL) under argon and heated at 70 °C in a sealed tube for 4 h. Concentration of the reaction mixture and addition of hexane afforded yellow crystals of **5** and orange crystals of **6**. Recrystallization from  $\text{CH}_2\text{Cl}_2$ /hexane gave pure **6** (30% yield). Mp: 167–169 °C dec. Anal. Calcd for  $\text{C}_{40}\text{H}_{36}\text{NO}_3\text{P}_2\text{RhS}_2 \cdot \text{CH}_2\text{Cl}_2$ : C, 55.17; H, 4.29; N, 1.57. Found: C, 55.27; H, 4.36; N, 1.60.

**X-ray Crystal Structure Determination of **5**.** Crystal data are summarized in Table I. X-ray measurements were carried out with a Rigaku AFC-5 four-circle diffractometer equipped with a graphite monochromator using  $\omega$ - $\theta$  scans and 10-s stationary background counts made at the lower and upper limits of each scan. A constant scan speed of  $0.06^\circ \text{ s}^{-1}$  was used. The data were corrected for Lorentz and polarization effects but not for absorption. A total of 7322 unique reflections in the ranges  $\pm h, \pm k, \pm l$  and  $2.8^\circ < 2\theta < 50^\circ$  were measured, of which 5751 independent reflections having  $I > 3\sigma(I)$  were used in subsequent analysis.

The structure was solved from direct and Fourier methods and refined by block-diagonal least squares with anisotropic thermal parameters in the last cycles for all non-hydrogen atoms. Hydrogen atoms for the six phenyl rings were placed in calculated positions, while those for the methyl groups and for the solvent of crystallization ( $\text{CH}_2\text{Cl}_2$ ) could not be located from a difference Fourier map. In the refinement, unit weights were applied. The function minimized in the least-squares refinement was  $\sum w(|F_o| - |F_c|)^2$ . The computational program package used in the analysis was the UNICS 3 program system.<sup>8</sup> Final  $R$  and  $R_w$  values were

Table II. Atomic Coordinates ( $\times 10^4$ ) for **5** with Estimated Standard Deviations in Parentheses

atom	x	y	z
Rh	243 (1)	2663 (1)	5641 (1)
Cl1	5811 (4)	1189 (4)	6655 (6)
Cl2	7344 (7)	1188 (5)	9353 (7)
P1	-1530 (2)	2968 (2)	4507 (3)
P2	1939 (2)	2209 (2)	6723 (3)
S1	1262 (3)	3425 (2)	4592 (3)
S2	-23 (2)	1863 (2)	3494 (3)
O1	-506 (8)	2790 (6)	8828 (9)
O2	-661 (7)	2126 (4)	6727 (8)
O3	424 (6)	3312 (4)	7560 (8)
N	1104 (9)	2596 (6)	2097 (10)
C1	-262 (10)	2750 (7)	7794 (12)
C2	845 (9)	2629 (7)	3227 (12)
C3	1784 (15)	3288 (9)	1867 (16)
C4	733 (14)	1859 (8)	1012 (14)
C11	-2115 (9)	3439 (6)	5721 (11)
C12	-3174 (10)	3112 (8)	5757 (13)
C13	-3575 (12)	3470 (9)	6712 (15)
C14	-2930 (13)	4147 (9)	7651 (15)
C15	-1874 (12)	4484 (8)	7641 (13)
C16	-1461 (11)	4125 (7)	6686 (12)
C21	-1562 (9)	3610 (6)	3298 (11)
C22	-1634 (11)	4385 (7)	3608 (12)
C23	-1579 (12)	4870 (7)	2687 (13)
C24	-1438 (11)	4582 (7)	1468 (12)
C25	-1357 (11)	3814 (8)	1140 (12)
C26	-1417 (10)	3327 (7)	2041 (11)
C31	-2653 (9)	2099 (6)	3459 (11)
C32	-2623 (11)	1371 (7)	3778 (14)
C33	-3483 (12)	711 (8)	2983 (16)
C34	-4396 (12)	762 (8)	1867 (15)
C35	-4438 (12)	1477 (10)	1555 (16)
C36	-3585 (11)	2151 (8)	2333 (14)
C41	2560 (10)	1755 (9)	5523 (13)
C42	3212 (11)	2234 (10)	4967 (15)
C43	3630 (13)	1864 (14)	4009 (16)
C44	3409 (16)	1037 (14)	3649 (17)
C45	2809 (16)	584 (12)	4213 (18)
C46	2387 (13)	931 (9)	5146 (15)
C51	3193 (9)	2906 (7)	8060 (12)
C52	3034 (11)	3552 (8)	8869 (14)
C53	4003 (14)	4039 (9)	9947 (18)
C54	5072 (13)	3884 (10)	10227 (17)
C55	5230 (11)	3259 (9)	9439 (15)
C56	4294 (10)	2760 (8)	8354 (13)
C61	1659 (10)	1431 (6)	7609 (12)
C62	2455 (11)	1342 (8)	8795 (14)
C63	2251 (13)	707 (9)	9398 (16)
C64	1222 (14)	171 (9)	8808 (19)
C65	403 (14)	254 (9)	7589 (21)
C66	615 (11)	876 (7)	7009 (16)
C70	7166 (15)	1584 (11)	7921 (20)

Table III. Selected Interatomic Distances (Å) and Angles (deg)

Distances			
Rh-O2	2.083 (8)	Rh-O3	2.071 (8)
Rh-S1	2.347 (3)	Rh-S2	2.346 (3)
Rh-P1	2.356 (3)	Rh-P2	2.398 (3)
C1-O1	1.213 (17)	C1-O2	1.335 (15)
C1-O3	1.318 (15)	C2-S1	1.712 (13)
C2-S2	1.720 (13)	C2-N	1.321 (17)
Angles			
P1-Rh-P2	174.0 (1)	O2-Rh-O3	63.3 (3)
S1-Rh-S2	73.7 (1)	S1-Rh-O3	109.7 (2)
S2-Rh-O2	113.3 (2)	Rh-O2-C1	92.5 (7)
Rh-O3-C1	93.6 (7)	Rh-S1-C2	88.1 (4)
Rh-S2-C2	88.0 (4)	O2-C1-O3	110.5 (11)
S1-C2-S2	110.2 (8)		

0.069 and 0.100, respectively. Further refinement was unsuccessful due to disorder in the region of the solvent molecule. Neutral-atomic scattering factors were taken from ref 9. Final atomic parameters for the

(7) O'Connor, C.; Gilbert, J. D.; Wilkinson, G. *J. Chem. Soc. A* 1969, 84.(8) Sakurai, T.; Kobayashi, K. *Rikagaku Kenkyusho Hokoku* 1979, 55, 69.

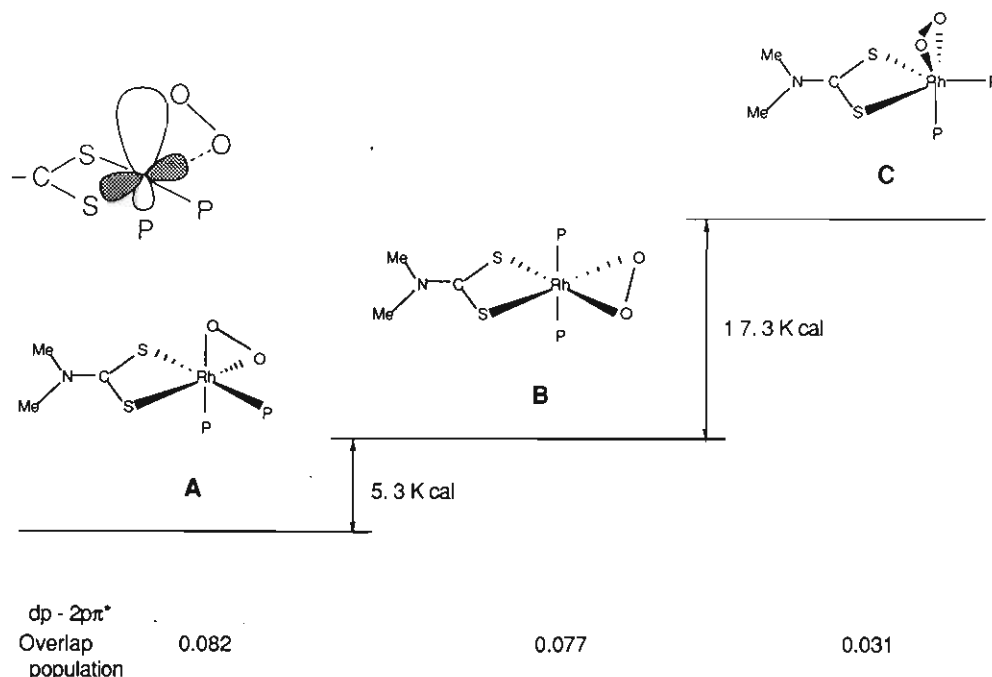


Figure 1. Structures of the dioxygen complexes (**2a,b**) and calculated overlap populations between Rh(dπ) and O<sub>2</sub>(2pπ\*).

Table IV. IR (cm<sup>-1</sup>) and NMR (ppm) Data

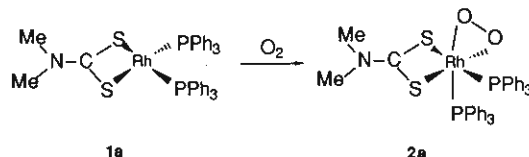
complex	IR	<sup>1</sup> H NMR		<sup>31</sup> P NMR	
		δ(Me)	δ(P)	J <sub>P-P</sub>	J <sub>Rh-P</sub>
<b>2a</b>	880 s	2.65, 2.84	26.05, 44.86	14.7	132, 143
<b>2b</b>	840 s	2.53, 2.74	55.32, 55.81	12.2	125, 119
<b>3a</b>	1665 s, 1630 sh	2.70, 3.02	17.98, 28.25	16.6	123, 124
<b>3b</b>	1650 s, 1630 sh	2.53, 2.74	55.32, 55.81	12.2	125, 119
<b>5</b>	1640 s, 1610 s	2.40	25.42		94
<b>6</b>	1650 w, 1610 s	2.67, 2.97			

non-hydrogen atoms and important bond lengths and angles are given in Tables II and III, respectively.

**Molecular Orbital Calculations.** The MO calculations were of the extended Hückel type<sup>10</sup> with the weighted  $H_{ij}$  formula.<sup>11</sup> The computational parameters for Rh<sup>12</sup> and other atoms<sup>13</sup> were taken from previous work. The Rh–ligand and intraligand bond lengths and angles were based on the crystal structure of **5**. The Rh–O and O–O distances were assumed to be 2.03 and 1.44 Å.<sup>14</sup>

## Results

**Dioxygen Complexes.** Rh(dtc)(PPh<sub>3</sub>)<sub>2</sub> (**1a**, dtc = dimethyldithiocarbamate) was first prepared by Wilkinson et al. by the equimolar reaction of chlorotris(triphenylphosphine)rhodium with sodium dimethyldithiocarbamate in acetone.<sup>7</sup> In our work, however, the reaction in THF proceeds much more easily. When dioxygen was bubbled through a benzene solution of **1a** at room temperature, brown fine crystals of the dioxygen adduct, Rh(dtc)(O<sub>2</sub>)(PPh<sub>3</sub>)<sub>2</sub> (**2a**), were isolated in 87% yield. Similarly,



Rh(dtc)(O<sub>2</sub>)(dppe) (**2b**, dppe = 1,2-bis(diphenylphosphino)ethane) was prepared from Rh(dtc)(dppe) (prepared in situ) and O<sub>2</sub>. IR

ν(O–O) absorptions listed in Table IV suggest coordination of the dioxygen is typical peroxy manner.<sup>15</sup> On the basis of the magnetic nonequivalence of the two methyl groups in the dtc ligand, as well as the presence of nonequivalent phosphine ligands (Table IV), structure A was assigned to these dioxygen adducts (Figure 1).

Extended Hückel MO calculations were carried out for structure A and the other possible structures B and C illustrated in Figure 1. In order to elucidate the nature of the metal–dioxygen bonding, the relative geometries between the metal–dioxygen and other metal–ligand bonds were fixed and only the arrangements of the ligands around the metal were varied. For instance, the Rh–O and O–O distances were 2.03 and 1.44 Å in all three models. Since the relative energy thus calculated indicates geometry A is the most stable of the three in agreement with the spectral observations, the present calculation may be valid. Previous MO studies on metal peroxy complexes suggest that the bonding between metals and dioxygen is similar to the Dewar model for metal olefin complexes with predominant π-bonding from filled metal d orbitals to the antibonding orbital of dioxygen.<sup>16</sup> The values for overlap population between metal dπ and dioxygen 2pπ\* orbitals are parallel to the relative energy, as listed in Figure 1, and suggest that back-donation from the metal to dioxygen is the determining factor also in the present case. Comparing structures A and B, we deduce that the P atom in phosphine can push filled metal d orbitals toward the ligand trans to it more effectively than the S atom in the dtc ligand does.

When **2a** and excess triphenylphosphine are dissolved in dichloromethane, phosphine oxide is formed and **1a** is regenerated. The oxidation of phosphine is much slower in benzene to allow recrystallization of **1a** from benzene/hexane.

**Peroxycarbonato and Carbonato Complexes.** When the <sup>1</sup>H NMR spectrum of **2a** was measured under an atmosphere of carbon dioxide, the two methyl peaks of **2a** instantaneously disappeared and new methyl peaks emerged at δ 2.70 and 3.02. A red complex (**3a**) having the same <sup>1</sup>H NMR absorptions was conveniently isolated by stirring a solution of **1a** under an atmosphere of a 1:1 mixture of O<sub>2</sub> and CO<sub>2</sub> at room temperature. The <sup>31</sup>P NMR spectrum of **3a** showed two different absorptions at δ 17.98 and 28.25. Elemental analysis is consistent with the

(9) *International Tables for X-Ray Crystallography*; Kynoch: Birmingham, England, 1976; Vol. 3, p 13.

(10) (a) Hoffmann, R. *J. Chem. Phys.* **1963**, *39*, 1397. (b) Hoffmann, R.; Lipscomb, W. N. *Ibid.* **1962**, *36*, 2179; *37*, 2872.

(11) Ammeter, J. H.; Bürgi, H.-B.; Thibeault, J. C.; Hoffmann, R. *J. Am. Chem. Soc.* **1978**, *100*, 3686.

(12) Thorn, D. L.; Hoffmann, R. *Nouv. J. Chim.* **1979**, *3*, 39.

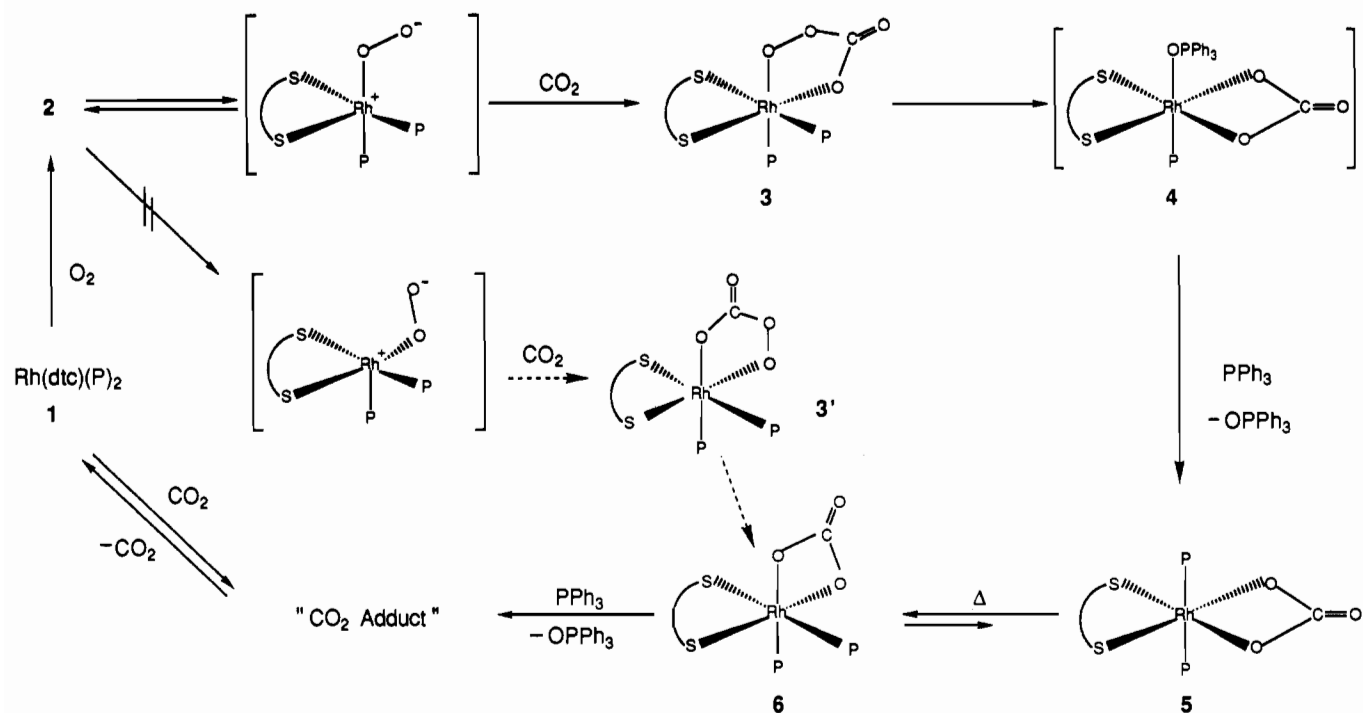
(13) Pinhas, A. R.; Hoffmann, R. *Inorg. Chem.* **1979**, *18*, 654.

(14) Laing, M.; Nolte, M. J.; Singleton, E. *J. Chem. Soc., Chem. Commun.* **1975**, 661.

(15) Mimoun, H. *Comprehensive Coordination Chemistry*; Pergamon Press: Oxford, England, 1987; Vol. 6, p 317.

(16) (a) Ziegler, T. *Inorg. Chem.* **1986**, *25*, 2721. (b) Norman, J. G.; Ryan, P. B. *Ibid.* **1982**, *21*, 3555. (c) Sakaki, S.; Hori, K.; Ohyoshi, A. *Ibid.* **1978**, *17*, 3183.

Scheme I



composition  $\text{Rh}(\text{dtc})(\text{CO}_4)(\text{PPh}_3)_2$ , and the structure illustrated in Scheme I was assigned to **3a**. The isomeric structure of peroxycarbonato complex **3a'** was unlikely according to the reaction mechanism described later.

Similarly, the *dpe* analogue of the peroxycarbonato complex **3b** was isolated, which also showed two different  $^1\text{H}$  NMR methyl absorptions at  $\delta$  2.53 and 2.74 and two different  $^{31}\text{P}$  absorptions at  $\delta$  55.32 and 55.81.

The platinum dioxygen complex  $\text{Pt}(\text{O}_2)(\text{PPh}_3)_2$  has been reported to react with  $\text{CO}_2$  to afford the peroxycarbonato complex, which was converted by excess  $\text{PPh}_3$  to the carbonato complex  $\text{Pt}(\text{CO}_3)(\text{PPh}_3)_2$  and  $\text{OPPh}_3$ .<sup>17</sup> Similarly, when a  $\text{CD}_2\text{Cl}_2$  solution of **3a** was allowed to stand at room temperature in the presence of four equimolar amounts of  $\text{PPh}_3$ , **3a** was gradually converted into the carbonato complex  $\text{Rh}(\text{dtc})(\text{CO}_3)(\text{PPh}_3)_2$  (**5**), producing phosphine oxide. The reaction, which was monitored by  $^1\text{H}$  and  $^{31}\text{P}$  NMR spectroscopy, was completed in 4 h. A more convenient way of preparing **5** is to stir a solution of **1a** and  $\text{PPh}_3$  under an atmosphere of  $\text{CO}_2/\text{O}_2$  for a prolonged time, without the isolation of **2a** and **3a**. Complex **5** was analyzed by means of X-ray crystallography to have a highly symmetric molecular configuration, as shown in Figure 2.

When a dichloromethane solution of the yellow carbonato complex **5** was heated at  $70^\circ\text{C}$  in the presence of triphenylphosphine, a new carbonato complex **6**, orange in color, was isolated by repeated recrystallization. The two *dtc* methyl groups in complex **6** are magnetically nonequivalent (Table IV), and the structure with *cis* triphenylphosphine ligands is assigned (Scheme I). In  $\text{CD}_2\text{Cl}_2$  solution at  $70^\circ\text{C}$ , **5** and **6** are in equilibrium, as monitored by  $^1\text{H}$  NMR spectroscopy, where **6** is thermodynamically more stable, the ratio **6/5** in the equilibrated mixture being about 2.

When this solution containing these isomeric carbonato complexes and excess triphenylphosphine was heated for a prolonged time, further clean change was observed, which was followed by  $^1\text{H}$  NMR spectroscopy. As the peaks due to **5** and **6** became smaller, new peaks appeared at  $\delta$  2.34 and 3.11 with an intensity ratio of about 5/1. The former of these two peaks is that of **1a**, and the latter is attributable to the "CO<sub>2</sub> adduct" of **1a** (see next section). Formation of phosphine oxide in this reaction was

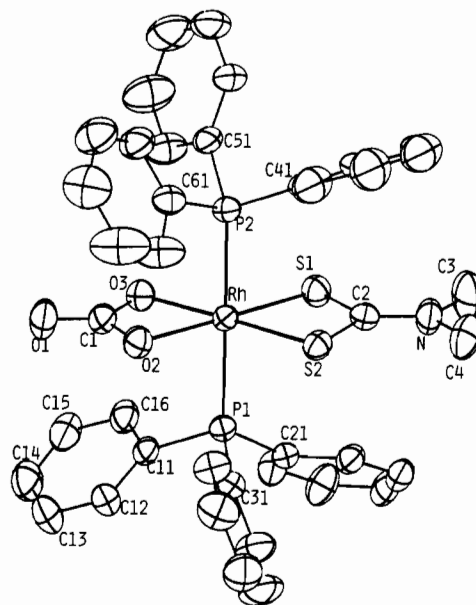


Figure 2. Molecular structure of **5** with atomic numbering scheme.

confirmed by the  $^{31}\text{P}$  NMR spectra.

**Interaction of Carbon Dioxide with  $\text{Rh}(\text{dtc})(\text{PPh}_3)_2$ .** Although isolation of a  $\text{CO}_2$  adduct of complex **1a** was unsuccessful, it was found that  $\text{CO}_2$  can interact with **1a** at atmospheric pressure. Thus an NMR sample of **1a** in  $\text{CD}_2\text{Cl}_2$  solution was sealed under an atmosphere of  $\text{CO}_2$ , which exhibited a new *dtc* methyl peak at  $\delta$  3.11 in the  $^1\text{H}$  NMR spectrum and a new phosphine peak at 48.50 in the  $^{31}\text{P}$  NMR spectrum. When the seal was opened and the sample flushed with argon before the tube was stoppered, the peak at  $\delta$  3.11 decreased dramatically and an intense peak for **1a** at  $\delta$  2.34 was regenerated. It appears, therefore, that **1a** forms a "CO<sub>2</sub> adduct" in solution that is stable only under an atmosphere of  $\text{CO}_2$ . The  $^1\text{H}$  and  $^{31}\text{P}$  NMR spectra suggest that this adduct has a symmetric structure.

#### Discussion

The reaction sequence described above and the reaction mechanism are summarized in Scheme I. In general,  $\eta^2$ -dioxygen (side-on) complexes of group VIII metal complexes can act as

(17) Hayward, P. J.; Blake, D. M.; Wilkinson, G.; Nyman, C. J. *J. Am. Chem. Soc.* **1970**, *92*, 5873.

1,3-dipolar  $M^+-O-O^-$  (end-on) complexes in their activated form. They are believed to be involved in the reaction of metal dioxygen complexes with both nucleophilic and electrophilic substrates.<sup>18</sup> In Co and Fe porphyrin complexes the end-on dioxygen complexes are more stable than the side-on form.<sup>19</sup> Starting from **2a** or **2b**, two isomers of end-on dioxygen intermediates are possible, depending on which Rh–O bond is cleaved. On the basis of the structures of peroxy-carbonato complexes **3a** and **3b**, we believe that the Rh–O bond trans to one of the Rh–S bonds opens and the Rh–O trans to the phosphine remains intact. This is in accord with the discussion based on MO calculations (vide supra) that phosphines can push filled metal d orbitals more effectively than the dithiocarbamate ligand can, enhancing back-donation from the metal to the ligand trans to phosphine.

We believe that the next step is attachment of the equatorial phosphine to the axial oxygen atom. The phosphine oxide thus

formed will weakly coordinate to the metal and blocks the axial position,<sup>20</sup> forcing the carbonato ligand to chelate at the equatorial site trans to the dtc ligand. Successive displacement of the phosphine oxide by free  $PPh_3$  will complete the formation of **5**. In agreement with this scheme, the peroxy-carbonato complex with the dppe ligand, **3b**, was found to be much more stable than **3a**, since its solution did not show any change in 4 h, while isolation of pure **3a** was often difficult due to its spontaneous transformation to **5**. If the isomeric peroxy-carbonato complex **3a'** was formed by the reaction of **2a** with  $CO_2$ , it should have given carbonato complex **6** directly. In reality, complex **6** was detected only when the kinetically formed carbonato complex **5** was isomerized by heating.

**Supplementary Material Available:** Listings of hydrogen atom parameters and temperature factors (2 pages); a table of calculated and observed structure factors (25 pages). Ordering information is given on any current masthead page.

- (18) (a) Broadhurst, M. J.; Brown, J. M.; John, R. A. *Angew. Chem., Int. Ed. Engl.* **1983**, *22*, 47. (b) Ugo, R.; Zanderighi, J. M.; Fusi, A.; Carreri, D. *J. Am. Chem. Soc.* **1980**, *102*, 3745 and references therein.  
 (19) (a) Rodley, G. A.; Robinson, W. T. *Nature* **1972**, *235*, 438. (b) Collman, J. P.; Halpert, T. R.; Suslick, K. S. *Metal Ion Activation of Dioxygen*; John Wiley & Sons: New York, 1980.

- (20) A binuclear iron- $\mu$ -dioxygen complex with triphenylphosphine oxide ligands has recently been reported: Sawyer, D. T.; McDowell, M. S.; Spencer, L.; Tsang, K. S. *Inorg. Chem.* **1989**, *28*, 1166.

Contribution from the Department of Chemistry,  
 University of South Carolina, Columbia, South Carolina 29208

## Cluster Synthesis. 28. New Platinum–Cobalt Carbonyl Cluster Complexes and Products Obtained from Their Reactions with Alkynes

Richard D. Adams,\* Gong Chen, Wengan Wu, and Jianguo Yin

Received March 27, 1990

The reaction of  $Pt(COD)_2$ , COD = 1,5-cyclooctadiene, with  $Co_2(CO)_8$  in cyclohexane solvent at 25 °C has yielded the new compounds  $PtCo_2(CO)_7(COD)$  (**1**, 3%) and  $Pt_2Co_2(CO)_8(COD)$  (**2**, 31%) and the known compound  $Co_4(CO)_{12}$  (**3**, 14%). Compounds **1** and **2** were characterized by single-crystal X-ray diffraction analyses. Compound **1** contains a triangular cluster of one platinum and two cobalt atoms with a carbonyl ligand bridging the Co–Co bond. Compound **2** consists of a tetrahedral cluster of two platinum atoms and two cobalt atoms. The Pt–Pt bond is weak, 2.9546 (6) Å. Compound **2** reacts with  $EtC_2Et$  to yield the new complex  $Pt_2Co_2(CO)_8(\mu_3-EtC_2Et)_2$  (**4**, 8%), and it reacts with  $PhC_2Ph$  to yield the new complex  $Pt_2Co_2(CO)_6(COD)_2(\mu_3-PhC_2Ph)_2$  (**5**, 22%). Compounds **4** and **5** were characterized crystallographically. Compound **4** contains a butterfly cluster of two cobalt and two platinum atoms. The two platinum atoms occupy the hinge positions and are joined by a short Pt–Pt bond, 2.4945 (7) Å. Triply bridging  $EtC_2Et$  ligands bridge the two  $Pt_2Co$  triangles. Compound **5** contains a bow-tie cluster of three platinum and two cobalt atoms with a platinum atom in the center. Triply bridging  $PhC_2Ph$  ligands bridge the two  $Pt_2Co$  triangular groupings. Crystallographic parameters for **1**: space group  $Pbca$ ,  $a = 15.076$  (3) Å,  $b = 16.298$  (3) Å,  $c = 14.547$  (5) Å,  $Z = 8$ ,  $R = 0.033$ , and  $R_w = 0.033$  for 2149 reflections. For **2**: space group  $P2_1/n$ ,  $a = 8.835$  (2) Å,  $b = 14.573$  (2) Å,  $c = 15.377$  (2) Å,  $\beta = 100.69$  (1)°,  $Z = 4$ ,  $R = 0.024$ , and  $R_w = 0.027$  for 2140 reflections. For **4**: space group  $P2_1/n$ ,  $a = 9.430$  (2) Å,  $b = 14.915$  (4) Å,  $c = 17.931$  (3) Å,  $\beta = 99.11$  (2)°,  $Z = 4$ ,  $R = 0.022$ , and  $R_w = 0.023$  for 2236 reflections. For **5**: space group  $C2/c$ ,  $a = 34.905$  (8) Å,  $b = 15.106$  (4) Å,  $c = 19.028$  (3) Å,  $\beta = 102.39$  (2)°,  $Z = 8$ ,  $R = 0.064$ , and  $R_w = 0.076$  for 3760 reflections.

### Introduction

Although platinum has many useful properties, its ability to promote a variety of chemical reactions catalytically is probably its most important.<sup>1,2</sup> Supported bimetallic clusters containing platinum are used commercially in the petroleum reforming process.<sup>2</sup> Because of this, there has been a great interest in the synthesis of heteronuclear cluster complexes containing platinum<sup>3</sup> and in their ability to produce catalysis.<sup>4</sup> Stone has shown that

the "ligand-free" platinum complexes are excellent reagents for the preparation of heteronuclear cluster complexes containing platinum.<sup>5</sup>

To date, there are only a few examples of cluster complexes that contain both cobalt and platinum,<sup>6–11</sup> but some of these have

- (1) (a) Speier, J. L. *Adv. Organomet. Chem.* **1979**, *17*, 407. (b) Kummer, J. T. *J. Phys. Chem.* **1986**, *90*, 4747. (c) Rylander, P. N. *Catalytic Hydrogenation Over Platinum Metals*; Academic Press: New York, 1967. (d) Zimmer, H.; Dobrovolszky, M.; Tétényi, P.; Paál, Z. *J. Phys. Chem.* **1986**, *90*, 4758 and references therein.  
 (2) (a) Sinfelt, J. H. *Bimetallic Catalysts*; Wiley: New York, 1983. (b) Sinfelt, J. H. *Acc. Chem. Res.* **1977**, *10*, 15.  
 (3) (a) Farrugia, L. J. *Adv. Organomet. Chem.*, in press. (b) Roberts, D. A.; Geoffroy, G. L. In *Comprehensive Organometallic Chemistry*; Wilkinson, G., Stone, F. G. A., Abel, E., Eds.; Pergamon: Oxford, England, 1982; Chapter 40.

- (4) Braunstein, P.; Rose, J. In *Stereochemistry of Organometallic and Inorganic Compounds*; Bernal, I., Ed.; Elsevier: Amsterdam, 1989; Vol. 3, pp 3–138.  
 (5) (a) Stone, F. G. A. *Acc. Chem. Res.* **1981**, *14*, 318. (b) Stone, F. G. A. *Inorg. Chim. Acta* **1981**, *50*, 33.  
 (6) Braunstein, P.; Dehand, J.; Nennig, J. F. *J. Organomet. Chem.* **1975**, *92*, 117.  
 (7) Bender, R.; Braunstein, P. *Nouv. J. Chim.* **1981**, *5*, 81.  
 (8) Barbier, J. P.; Braunstein, P.; Fischer, J.; Ricard, L. *Inorg. Chim. Acta* **1978**, *31*, L361.  
 (9) Bender, R.; Braunstein, P.; Metz, B.; Lemoine, P. *Organometallics* **1984**, *3*, 381.  
 (10) (a) Braunstein, P.; de Meric de Bellefon, C.; Reis, M. *Inorg. Chem.* **1988**, *27*, 1338. (b) Braunstein, P.; Dehand, J. *Bull. Soc. Chim. Fr.* **1975**, 1997.